

Partial Wave Analysis of $J/\psi \rightarrow \gamma(K^+K^-\pi^+\pi^-)$

J. Z. Bai,¹ Y. Ban,⁶ J. G. Bian,¹ A. D. Chen,¹ G. P. Chen,¹ H. F. Chen,² H. S. Chen,¹
 J. C. Chen,¹ X. D. Chen,¹ Y. Chen,¹ Y. B. Chen,¹ B. S. Cheng,¹ X. Z. Cui,¹ H. L. Ding,¹
 L. Y. Dong,^{1,8} Z. Z. Du,¹ C. S. Gao,¹ M. L. Gao,¹ S. Q. Gao,¹ J. H. Gu,¹ S. D. Gu,¹
 W. X. Gu,¹ Y. N. Guo,¹ Z. J. Guo,¹ S. W. Han,¹ Y. Han,¹ J. He,¹ J. T. He,¹ K. L. He,¹
 M. He,³ Y. K. Heng,¹ G. Y. Hu,¹ H. M. Hu,¹ J. L. Hu,¹ Q. H. Hu,¹ T. Hu,¹ G. S. Huang,^{1,8}
 X. P. Huang,¹ Y. Z. Huang,¹ C. H. Jiang,¹ Y. Jin,¹ X. Ju,¹ Z. J. Ke,¹ Y. F. Lai,¹
 P. F. Lang,¹ C. G. Li,¹ D. Li,¹ H. B. Li,^{1,8} J. Li,¹ J. C. Li,¹ P. Q. Li,¹ W. Li,¹ W. G. Li,¹
 X. H. Li,¹ X. N. Li,¹ X. Q. Li,⁹ Z. C. Li,¹ B. Liu,¹ F. Liu,⁷ Feng Liu,¹ H. M. Liu,¹, J. Liu,¹
 J. P. Liu,¹¹ R. G. Liu,¹ Y. Liu,¹ Z. X. Liu,¹ G. R. Lu,¹⁰ F. Lu,¹ J. G. Lu,¹ X. L. Luo,¹
 E. C. Ma,¹ J. M. Ma,¹ H. S. Mao,¹ Z. P. Mao,¹ X. C. Meng,¹ X. H. Mo,¹ J. Nie,¹ N. D. Qi,¹
 X. R. Qi,⁶ C. D. Qian,⁵ J. F. Qiu,¹ Y. H. Qu,¹ Y. K. Que,¹ G. Rong,¹ Y. Y. Shao,¹
 B. W. Shen,¹ D. L. Shen,¹ H. Shen,¹ H. Y. Shen,¹ X. Y. Shen,¹ F. Shi,¹ H. Z. Shi,¹
 X. F. Song,¹ H. S. Sun,¹ L. F. Sun,¹ Y. Z. Sun,¹ S. Q. Tang,¹ G. L. Tong,¹ F. Wang,¹
 L. Wang,¹ L. S. Wang,¹ L. Z. Wang,¹ P. Wang,¹ P. L. Wang,¹ S. M. Wang,¹ Y. Y. Wang,¹
 Z. Y. Wang,¹ C. L. Wei,¹ N. Wu,¹ Y. G. Wu,¹ D. M. Xi,¹ X. M. Xia,¹ Y. Xie,¹ Y. H. Xie,¹
 G. F. Xu,¹ S. T. Xue,¹ J. Yan,¹ W. G. Yan,¹ C. M. Yang,¹ C. Y. Yang,¹ H. X. Yang,¹
 X. F. Yang,¹ M. H. Ye,¹ S. W. Ye,² Y. X. Ye,² C. S. Yu,¹ C. X. Yu,¹ G. W. Yu,¹ Y. H. Yu,⁴
 Z. Q. Yu,¹ C. Z. Yuan,¹ Y. Yuan,¹ B. Y. Zhang,¹, C. Zhang,¹ C. C. Zhang,¹ D. H. Zhang,¹
 Dehong Zhang,¹ H. L. Zhang,¹ J. Zhang,¹ J. W. Zhang,¹ L. Zhang,¹ Lei Zhang,¹
 L. S. Zhang,¹ P. Zhang,¹ Q. J. Zhang,¹ S. Q. Zhang,¹ X. Y. Zhang,³ Y. Y. Zhang,¹
 D. X. Zhao,¹ H. W. Zhao,¹ Jiawei Zhao,² J. W. Zhao,¹ M. Zhao,¹ W. R. Zhao,¹
 Z. G. Zhao,¹ J. P. Zheng,¹ L. S. Zheng,¹ Z. P. Zheng,¹ B. Q. Zhou,¹ L. Zhou,¹ K. J. Zhu,¹
 Q. M. Zhu,¹ Y. C. Zhu,¹ Y. S. Zhu,¹ Z. A. Zhu,¹ B. A. Zhuang,¹

(BES Collaboration)[†]

D. V. Bugg¹² and B. S. Zou^{1,12}

¹ *Institute of High Energy Physics, Beijing 100039, People's Republic of China*

² *University of Science and Technology of China, Hefei 230026, People's Republic of China*

³ *Shandong University, Jinan 250100, People's Republic of China*

⁴ *Hangzhou University, Hangzhou 310028, People's Republic of China*

⁵ *Shanghai Jiaotong University, Shanghai 200030, People's Republic of China*

⁶ *Peking University, Beijing 100871, People's Republic of China*

⁷ *Hua Zhong Normal University, Wuhan 430079, People's Republic of China*

⁸ *China Center for Advanced Science and Technology(CCAST), World Laboratory, Beijing 100080, People's Republic of China)*

⁹ *Nankai University, Tianjin 300071, People's Republic of China*

¹⁰ *Henan Normal University, Xinxiang 453002, People's Republic of China*

¹¹ *Wuhan University, Wuhan 430072, People's Republic of China*

¹² *Queen Mary and Westfield College, London E1 4NS, United Kingdom*

Abstract

BES data on $J/\psi \rightarrow \gamma(K^+K^-\pi^+\pi^-)$ are presented. The $K^*\bar{K}^*$ contribution peaks strongly near threshold. It is fitted with a broad 0^{-+} resonance with mass $M = 1800 \pm 100$ MeV, width $\Gamma = 500 \pm 200$ MeV. A broad 2^{++} resonance peaking at 2020 MeV is also required with width ~ 500 MeV. There is further evidence for a 2^{-+} component peaking at 2.55 GeV. The non- $K^*\bar{K}^*$ contribution is close to phase space; it peaks at 2.6 GeV and is very different from $K^*\bar{K}^*$.

PACS numbers: 14.40.Cs, 12.39.Mk, 13.25.Jx, 13.40.Hq

Typeset using REVTeX

In 1990, MARK III presented their spin-parity analysis of $J/\psi \rightarrow \gamma K^* \bar{K}^*$ at the Rheinfels Workshop on the Hadron Mass Spectrum [1]. They found a dominant 0^{-+} component, accounting for 55% of the data. In addition, smaller 2^+ and 2^- channels of about equal strength were observed. Interferences were not included. Here we present BES data and carry out a full partial wave analysis.

Lattice QCD and other theoretical models predict 0^{-+} and 2^{++} glueballs with masses 2.0 to 2.4 GeV [2]. Recently, several broad structures have been identified in this mass range. In an analysis of Mark III data on radiative decays of J/ψ to $\eta\pi^+\pi^-$, $\rho\rho$, $\omega\omega$, $K^*\bar{K}^*$ and $\phi\phi$, a very broad 0^- component has been found [3] with a mass of 1750–2190 MeV and a width of order 1 GeV. Its decays are flavour blind to first approximation, making it a candidate for the 0^- glueball. This 0^- component appears strongly in BES data on $J/\psi \rightarrow \gamma(\pi^+\pi^-\pi^+\pi^-)$ [4]. There, we also find a broad 2^+ contribution fitted as a resonance at 1940 ± 60 MeV with $\Gamma = 350 \pm 100$ MeV. The WA91 and WA102 groups have also found a broad 2^+ resonance at 1920 MeV in their 4π mass spectrum [5]. A recent partial wave analysis of Crystal Barrel data on $p\bar{p} \rightarrow \eta\eta\pi^0$ [6] has found a broad $f_2(1980) \rightarrow \eta\eta$ resonance with mass 1980 MeV and width 500 MeV. There are further data on $\bar{p}p \rightarrow \eta\pi^0\pi^0$ [7,8], where a broad 0^- component is observed plus a peak in $\eta\sigma$ at 2140 MeV with width ~ 150 MeV. In Refs. [3] and [4], an $f_0(2100)$ was observed in 4π states. A peak at this mass was observed earlier in the E760 experiment [9]. The $f_0(2100)$ decay to $\eta\eta$ has been confirmed in two sets of Crystal Barrel data [10,11].

The analysis in this paper uses 7.8×10^6 J/ψ triggers collected by the Beijing Spectrometer(BES). This detector has been described in detail in Ref [12]. Here we describe briefly those detector elements crucial to this measurement. Tracking is provided by a 10 superlayer main drift chamber (MDC). Each superlayer contains four layers of sense wires measuring both the position and the ionization energy loss (dE/dx) of charged particles. The momentum resolution is $\sigma_P/P = 1.7\%\sqrt{1+P^2}$, where P is the momentum of charged tracks in GeV/ c . The resolution of the dE/dx measurement is about 9%. This provides good π/K separation and proton identification in the low momentum region. An array of 48

scintillation counters surrounding the MDC measures the time-of-flight (TOF) of charged tracks with a resolution of $330ps$ for hadrons. Outside the TOF system is an electromagnetic calorimeter composed of streamer tubes and lead sheets with a z positional resolution of 4 cm. The energy resolution scales as $\sigma_E/E = 22\%/\sqrt{E}$, where E is the energy in GeV. Outside the shower counter is a solenoidal magnet producing a 0.4 Tesla magnetic field.

Each candidate event is required to have exactly four charged tracks. Every track must have a good helix fit in the polar angle range $-0.8 < \cos \theta < 0.8$ and a transverse momentum > 60 MeV/c. A vertex is required within an interaction region ± 20 cm longitudinally and 2 cm radially. At least one reconstructed γ is required in the barrel shower counter. A minimum energy cut of 80 MeV is imposed on the photons. Showers associated with charged tracks are also removed.

A positive identification of at least one K^\pm and one π^\pm is required using time of flight and/or dE/dx . If two tracks are ambiguous, both alternative identifications are tried. Events are fitted kinematically to the 4C hypothesis $J/\psi \rightarrow \gamma(K^+K^-\pi^+\pi^-)$, requiring a confidence level $> 5\%$. If there is more than one photon, the fit is repeated using all permutations. Events with two or more photons are also fitted to $J/\psi \rightarrow \gamma\gamma K^+K^-\pi^+\pi^-$. Those giving a better fit than to $\gamma(K^+K^-\pi^+\pi^-)$ are rejected, as are events fitting the final state $K^+K^-\pi^+\pi^-$. Next, we require $|U_{miss}| = |E_{miss} - P_{miss}| < 0.12$ GeV/c², so as to reject the events with multi-photons or more or less than two charged kaons; here, E_{miss} and P_{miss} are, respectively, the missing energy and missing momentum of all charged particles; they are calculated by assuming the charged particles are $K^+K^-\pi^+\pi^-$. The momentum of the $K^+K^-\pi^+\pi^-$ system transverse to the photon $P_{t\gamma}^2 = 4 |P_{miss}|^2 \sin^2(\theta_{m\gamma}/2) < 0.006$ (GeV/c)² is required in order to remove the background $J/\psi \rightarrow \pi^0 K^+K^-\pi^+\pi^-$; here $\theta_{m\gamma}$ is the angle between the missing momentum and the photon direction. Finally, to remove a small background of K_s^0 , we perform a cut on the $\pi^+\pi^-$ invariant mass, $|M_{\pi^+\pi^-} - M_{K_s^0}| > 25$ MeV; to remove the small background due to $\phi(1020)$, we use a cut on the K^+K^- invariant mass, $|M_{K^+K^-} - M_\phi| > 20$ MeV; background $J/\psi \rightarrow \omega K^+K^-$ events are eliminated by the cut $|M_{\pi^+\pi^-\pi^0} - M_\omega| > 25$ MeV, in fitting the $\pi^0 K^+K^-\pi^+\pi^-$ hypothesis with only one

photon detected and the π^0 associated to the missing momentum. The number of surviving events is 1516.

The effects of the various selection cuts on the data is simulated with a full Monte Carlo of the BES detector; 500,000 Monte Carlo events are successfully fitted to $J/\psi \rightarrow \gamma(K^+K^-\pi^+\pi^-)$; all background reactions are similarly fitted to this channel. The estimated background is 16%, purely from $J/\psi \rightarrow \pi^0(K^+K^-\pi^+\pi^-)$. We have included this background in the amplitude analysis, but it lies very close to non- $K^*\bar{K}^*$ events and has negligible effect on the analysis of $K^*\bar{K}^*$ events.

Fig. 1 shows the KK , $\pi\pi$, $K\pi$, $KK\pi$, K^*K and $K^*\pi$ invariant mass distributions of selected events after acceptance cuts. These cuts are accomodated in the maximum likelihood fit, using the full Monte Carlo simulation of the detector. A strong K^* signal is clearly visible. There is just a hint of possible structure in Fig. 1(a) around 1500 MeV, but including $f_0(1500)$ or $f'_2(1525)$ into the fit fails to reveal any significant contribution. It is too narrow for $f'_2(1525)$. Figs. 1(e) and (f) show no significant structure attributable to heavier K_1 or K^* 's states. The $K^+K^-\pi^+\pi^-$ invariant mass distribution of $J/\psi \rightarrow \gamma K^+K^-\pi^+\pi^-$ is shown in Fig. 2(a). The $K^*\bar{K}^*$ mass spectrum is obtained with a double cut on the two $K\pi$ invariant masses, $|M_{K\pi} - M_{K^*}| < 75$ MeV and is shown in Fig. 2(b). Fig. 3(a) shows the $K^+K^-\pi^+\pi^-$ mass spectrum of $J/\psi \rightarrow \gamma K^+K^-\pi^+\pi^-$ when one $K\pi$ or both $K\pi$ masses fall outside the K^* region.

We first attempted to fit the non- $K^*\bar{K}^*$ data of Fig. 3(a) as $\kappa\kappa$ and $K^{*0}\kappa + c.c.$; here κ means the $K\pi$ S-wave. The κ is parametrized to fit LASS data [13] on $K_0^*(1430)$. Each κ is made from $K^+\pi^-$ or $K^-\pi^+$, and if the κ really dominates this process, the $K\pi$ mass distribution should follow it. The dashed curve in Fig. 3(b) shows that this fails.

A simple solution which works well is to fit instead with $K^+K^-\pi^+\pi^-$ phase space. This is shown by the full curve of Fig. 3(b). A detailed study of non- $K^*\bar{K}^*$ events reveals only a weak $\rho(770)$ signal, visible in Fig. 1(b). However, when we perform a cut on the $\pi^+\pi^-$ mass: $|M_{\pi\pi} - M_\rho| < 100$ MeV, we have been unable to correlate this signal with any particular K^+K^- , $K^\pm\pi^+\pi^-$ or $K^+K^-\pi^+\pi^-$ resonance.

We now turn to $K^*\bar{K}^*$ events. One sees immediately a large difference between $K^*\bar{K}^*$ and non- $K^*\bar{K}^*$ events from Fig. 2(b) and 3(a). The $K^*\bar{K}^*$ events peak strongly close to threshold. We shall show that the data require a strong 0^- peak at threshold.

The amplitudes in the PWA analysis are constructed from Lorentz-invariant combinations of the 4-vectors and the photon polarization for J/ψ initial states with helicity ± 1 . Cross sections are summed over photon polarizations. The relative magnitudes and phases of the amplitudes are determined by a maximum likelihood fit. We use ℓ to denote the orbital angular momentum between the photon and $KK\pi\pi$ states in the production reaction. Because this is an electromagnetic transition, the same phase is used for amplitudes with different ℓ but otherwise the same final state. In fitting $K^*\bar{K}^*$, spin-parity assignments up to $J = 4$ have been tried.

We have examined slices of the $K^*\bar{K}^*$ mass spectrum ~ 200 MeV wide. Each slice has been fitted with a constant contribution with quantum numbers 0^{++} , 0^{-+} , 1^{++} , 2^{++} , 2^{-+} and 4^{++} . These different quantum numbers give angular distributions which are distinctively different. They depend on two angles (a) θ_{K^+} or θ_{π^+} of K^+ or π^+ with respect to the $K^+\pi^-$ or $K^-\pi^+$ pair in their rest frame, and (b) the azimuthal angle χ between the planes of $K^+\pi^-$ and $K^-\pi^+$ in the rest frame of the resonance. Results of the slice fit are shown in Fig. 4. The 0^{-+} contribution is largest and peaks towards the low mass end. There is evidence for a broad 2^{++} contribution peaking at ~ 2050 MeV, and this will be confirmed below by detailed fits. Contributions from 0^{++} and 4^{++} are small or absent. Though the results of the slice fit show that there may be some 1^{++} contributions in the $2.0 \sim 2.4$ GeV mass region and some 2^{-+} contributions at low mass, there is some degree of cross-talk with 0^- and 2^+ signals; when we put 1^{++} or 2^{-+} into the full fit in these regions, their contributions are found to be negligible and are absorbed into 0^- or 2^+ . At high masses, there is some evidence for a 2^{-+} contribution.

The precise mass dependence of each contribution is hard to establish because signals are broad and are affected by systematic uncertainties as follows. (a) There is an unknown form factor for the vertex $J/\psi \rightarrow \gamma X$. For consistency with other work, we adopt a very weak

form factor $\exp(-\alpha_g q^2)$ with $\alpha_g = 0.13 \text{ GeV}^{-2}$, fitted to many channels of J/ψ radiative decay [14]; q is the photon momentum in the J/ψ rest frame. (b) Likewise we use a form factor $\exp(-\alpha_d p^2)$ with $\alpha_d = 2.0 \text{ GeV}^{-2}$, where p is the momentum of the final K^* in the rest frame of X ; (c) The resonance X may couple to further channels at higher mass; this would pull the cross section down when these channels open. The effect of these form factors is to allow shifts of $\pm 50 \text{ MeV}$ in the mass fitted to the broad component; however, fitted intensities hardly change in shape at all.

We begin by fitting simple Breit-Wigner resonances of constant width to channels 0^{-+} , 2^{++} and 2^{-+} , including the form factors discussed above. Appropriate Blatt-Weisskopf centrifugal barrier factors are included with a radius consistent with the α parameters. The best fit is shown on Fig. 5. Crosses are data and histograms the fit.

The optimum mass for the broad 0^- contribution is $1800 \pm 100 \text{ MeV}$. The width optimises at $500 \pm 200 \text{ MeV}$. The present fit with a simple Breit-Wigner form is likely to be an over-simplification for such a broad state. In Ref. [14], all radiative decays are fitted simultaneously. This produces a slightly broader peak, shown by the dashed curve in Fig. 5(b), but with little effect on other components.

The 2^+ contribution of Fig. 5(c) is definitely required. Without it, log likelihood gets worse by 58; this is roughly an 8σ effect, from tables of log likelihood for 6 fitted parameters. The 2^- contribution is less secure. It improves log likelihood by 18.9 ($\sim 4.7\sigma$). Both the 2^- and 0^- contributions are produced in a P-wave and consequently vary as q^3 , where q is the momentum of the photon; this dependence leads to a slight underfit at the highest masses. If this defect is real, it is most likely fitted by a small E1 cross section for production of high mass 0^+ or 2^+ components, which cannot be identified definitively.

The broad 2^+ component near 2 GeV is interesting. It is very close to that required to fit BES data on $J/\psi \rightarrow \gamma(\pi^+\pi^-\pi^+\pi^-)$. It peaks at 2020 MeV. Because the $K^* \bar{K}^*$ phase space opens rapidly, the pole position tends to come out lower, around 1900 MeV with a width of 500 MeV. Changing the form factors moves the pole position up or down slightly, but leaves the fitted intensity almost unchanged.

Figs. 6(a) and (b) shows fitted angular distributions, summed over all $K^*\bar{K}^*$ masses. Figs. 6(c) and (d) illustrate angular distributions from individual quantum numbers. The necessity for a large 0^- contribution is obvious. The full angular dependence involves correlations between θ and χ (defined earlier), containing much more information than the projections of Fig. 6.

No significant 0^{++} , 1^{++} or 4^{++} resonance is found in the full fit (changes in log likelihood < 2.5). That result is itself interesting. There is no evidence for the $f_0(2100)$, which appears strongly in $J/\psi \rightarrow \gamma(4\pi)$ and also in two sets of Crystal Barrel data in the $\eta\eta$ channel and also in E760 data. Its absence from the present data suggests it is not an $s\bar{s}$ state.

Table I summarises branching ratios evaluated from the fit; the first error is statistical and the second covers systematic errors in the overall normalisation of the number of J/ψ interactions. The η_c component will be the subject of a separate publication, and has been subtracted. We find 1516 $KK\pi\pi$ events (of which 320 are $K^*\bar{K}^*$) within the cuts we have applied. For each K^* , 17.5% of events lie outside cuts. We correct branching ratios to allow for this loss. We also correct for all charges in $K^*\bar{K}^*$ channels: we have multiplied values obtained here by a factor (1.5^2) for Clebsch-Gordan coefficients in K^* decay and a further factor 2 for production of $K^{*+}\bar{K}^{*-}$ in the radiative decay process.

We have also searched for a 2^- contribution. A component with these quantum numbers was found in $J/\psi \rightarrow \gamma(\eta\pi^+\pi^-)$ at 1840 MeV [15]. A possible interpretation is as an $I = 0$ hybrid; an $s\bar{s}g$ hybrid is then to be expected around 2.1 GeV with roughly half the branching ratio, summed over all kaonic channels. We find that such a 2^- component with width 250–400 MeV produces only an insignificant improvement in the fit: an improvement in log likelihood of 4.5 for 4 extra parameters. The branching ratio for production and decay of the fitted 2^- component, corrected for all charge states, is then 1.8×10^{-4} . This is to be compared with the value $(9.3 \pm 3.33) \times 10^{-4}$ observed in all $\eta\pi\pi$ channels.

We summarize as follows. We fit with a broad 0^{-+} resonance with $M = 1800 \pm 100$ MeV and $\Gamma = 500 \pm 200$ MeV, decaying to $K^*\bar{K}^*$. It is to be identified with the broad 0^- component found also in $\eta\pi^+\pi^-$, $\rho\rho$, $\omega\omega$ and $\phi\phi$. The data also definitely required a broad

2^{++} resonance $f_2(1950)$ decaying to K^*K^* . The fit to the high mass end of the $K^+K^-\pi^+\pi^-$ spectrum is best achieved with an additional 2^{-+} signal.

The BES group thanks the staff of IHEP for technical support in running the experiment. This work is supported in part by China Postdoctoral Science Foundation and National Natural Science Foundation of China under contract Nos. 19991480, 19825116 and 19605007; and by the Chinese Academy of Sciences under contract No. KJ 95T-03(IHEP). We also acknowledge financial support from the Royal Society for collaboration between Chinese and UK groups.

REFERENCES

- † Data analyzed were taken prior to the participation of U.S. members of the BES Collaboration.
- [1] G. Eigen, CALT-68-1698, and Rheinfels Workshop on the Hadron Mass Spectrum, St. Goar, September 3-6, 1990.
 - [2] G.S. Bali *et al.*, Phys. Lett. **B 309** (1993) 378.
 - [3] D.V. Bugg and B.S. Zou, Phys. Lett. **B 396** (1997) 295.
 - [4] J.Z. Bai *et al.*, submitted to Phys. Lett. B.
 - [5] F. Antinori *et al.*, Phys. Lett. **B 353** (1995) 589;
D. Barberis *et al.*, Phys. Lett. **B 397** (1997) 339.
 - [6] D.V. Bugg, Nucl. Phys. **A 655** (1999) 57c;
A. Anisovich *et al.*, Phys. Lett. **B 449** (1999) 145.
 - [7] B.S. Zou, Nucl. Phys. **A 655** (1999) 41c.
 - [8] A. Anisovich *et al.*, Phys. Lett. **B 452** (1999) 180.
 - [9] T.A. Armstrong *et al.*, Phys. Lett. **B 307** (1993) 394.
 - [10] A. Anisovich *et al.*, submitted to Phys. Lett. **B**.
 - [11] A. Anisovich *et al.*, submitted to Phys. Lett. **B**.
 - [12] BES Collaboration, Nucl. Instr. Methods, **A 344** (1994) 319.
 - [13] D. Aston *et al.*, Nucl. Phys. **B 296** (1988) 493.
 - [14] D.V. Bugg, L.Y. Dong and B.S. Zou, Phys. Lett. **B 458** (1999) 511.
 - [15] J.Z. Bai *et al.*, Phys. Lett. **B 446** (1999) 356.

FIGURES

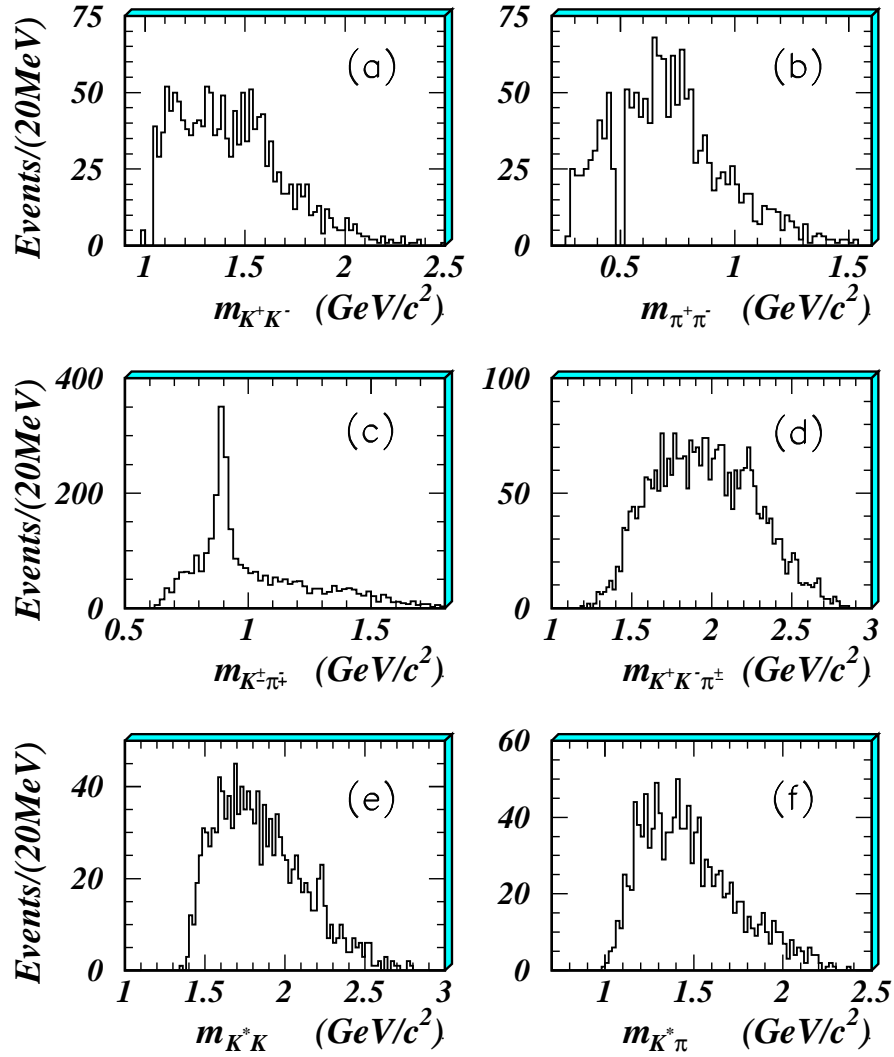


FIG. 1. The KK , $\pi\pi$, $K\pi$ (two entries/event), $KK\pi$ (two entries/event), K^*K and $K^*\pi$ masses of $J/\psi \rightarrow \gamma(K^+K^-\pi^+\pi^-)$.

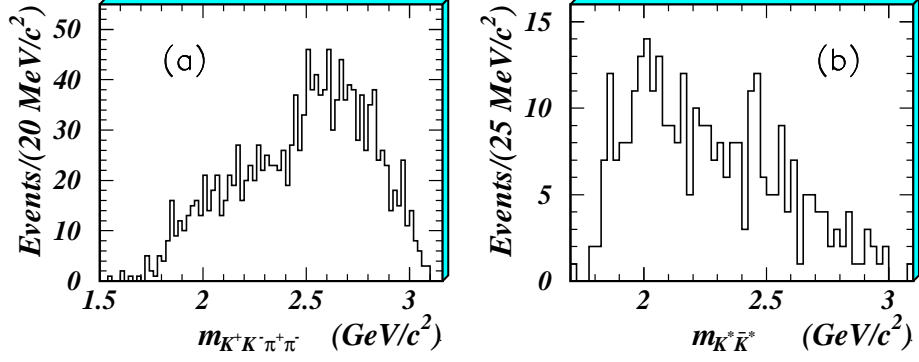


FIG. 2. (a) The $KK\pi\pi$ mass of $J/\psi \rightarrow \gamma K^+ K^- \pi^+ \pi^-$; (b) The $K^* \bar{K}^*$ mass of $J/\psi \rightarrow \gamma K^* \bar{K}^*$

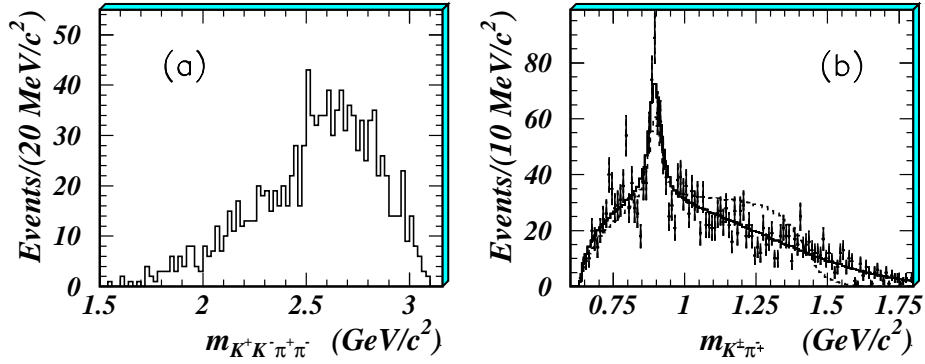


FIG. 3. The (a) $KK\pi\pi$ and (b) $K\pi$ mass spectrum from non- $K^* \bar{K}^*$ events. In (b), the dashed line shows the κ fitted to $K_0^*(1430)$ and the full line is derived from $K^+ K^- \pi^+ \pi^-$ phase space plus a fit to $K^* + K\pi$ phase space.

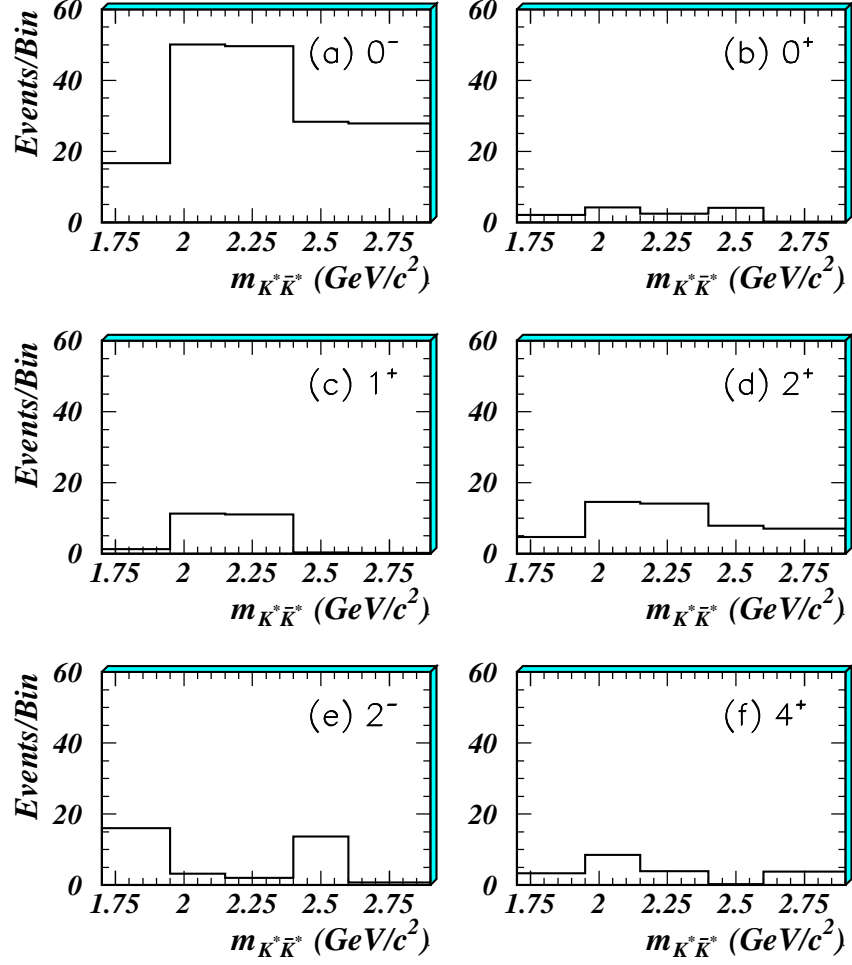


FIG. 4. The contribution of (a) 0^- , (b) 0^+ , (c) 1^+ , (d) 2^+ , (e) 2^- and (f) 4^+ from the slice fit to $J/\psi \rightarrow \gamma K^* \bar{K}^*$

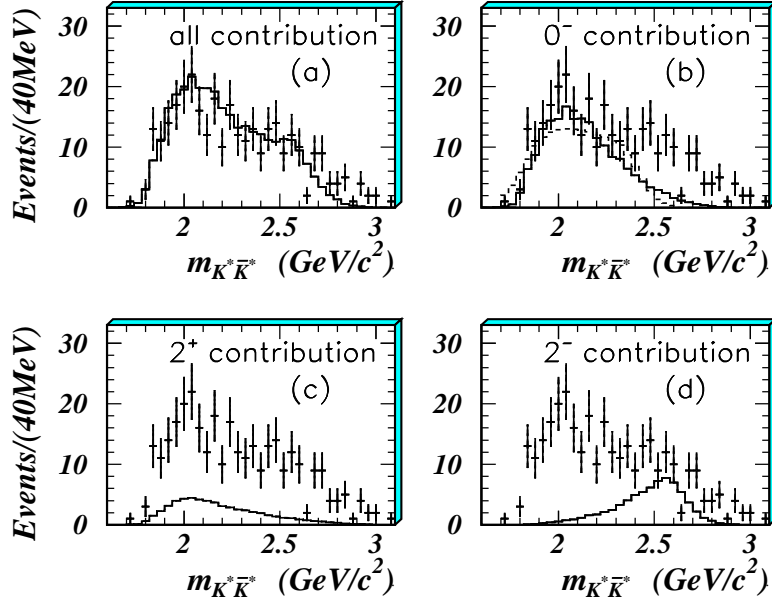


FIG. 5. Comparison of the mass spectrum of $K^* \bar{K}^*$ with (a) all, (b) 0^- , (c) 2^+ and (d) 2^- contributions from the best fit; the dashed curve shows the 0^- component fitted to the broad 0^- resonance in Ref. [14].

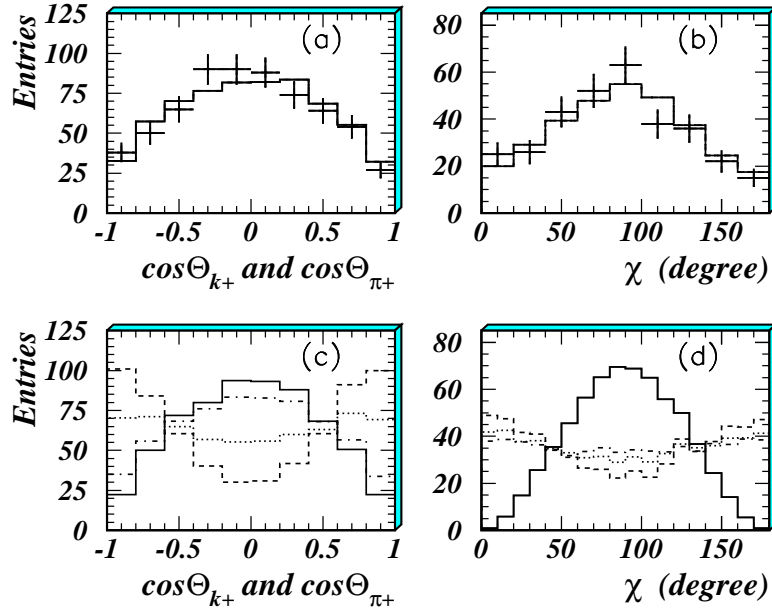


FIG. 6. (a) Comparison of $J/\psi \rightarrow \gamma K^* \bar{K}^*$ data and fit for (a) $\cos \theta_{K^+} + \cos \theta_{\pi^+}$ (both entries summed) and (b) χ ; (c) and (d) corresponding angular distributions for 0^- (full histograms), 0^+ (dashed), 2^+ (dotted) and 2^- (dash-dot).

TABLES

TABLE I. Branching ratios (BR) integrated over all masses, but excluding the η_c .

Channel	BR
$BR(J/\psi \rightarrow \gamma K^+ K^- \pi^+ \pi^-)$	$(2.1 \pm 0.1 \pm 0.6) \times 10^{-3}$
$BR(J/\psi \rightarrow \gamma K^* \bar{K}^*)$	$(4.0 \pm 0.3 \pm 1.3) \times 10^{-3}$
$BR(J/\psi \rightarrow \gamma 0^-) \times BR(0^- \rightarrow K^* \bar{K}^*)$	$(2.3 \pm 0.2 \pm 0.7) \times 10^{-3}$
$BR(J/\psi \rightarrow \gamma f_2(1950)) \times BR(f_2(1950) \rightarrow K^* \bar{K}^*)$	$(0.7 \pm 0.1 \pm 0.2) \times 10^{-3}$
$BR(J/\psi \rightarrow \gamma 2^-) \times BR(2^- \rightarrow K^* \bar{K}^*)$	$(0.9 \pm 0.1 \pm 0.3) \times 10^{-3}$